Original Article

Identification of gastric schwannoma and non-metastatic gastric stromal tumor by CT: a single-institution retrospective diagnostic test

Xiaolong Gu, Yang Li, Gaofeng Shi

Department of Radiology, The Fourth Hospital of Hebei Medical University, Shijiazhuang, China

Contributions: (I) Conception and design: X Gu; (II) Administrative support: G Shi; (III) Provision of study materials or patients: Y Li; (IV) Collection and assembly of data: X Gu; (V) Data analysis and interpretation: Y Li; (VI) Manuscript writing: All authors; (VII) Final approval of manuscript: All authors.

Correspondence to: Gaofeng Shi. Department of Radiology, The Fourth Hospital of Hebei Medical University, 12 Jiankang Road, Shijiazhuang 050000, China. Email: gaofengs62@sina.com.

Background: Gastric schwannoma (GS) was a rare mesenchymal tumor that was difficult to distinguish from a non-metastatic gastric stromal tumor (GST). The nomogram constructed by CT features had an advantage in the differential diagnosis of gastric malignant tumors. Therefore, we conducted a retrospective analysis of their respective computed tomography (CT) features.

Methods: We conducted a retrospective single-institution review of resected GS and non-metastatic GST between January 2017 and December 2020. Patients who were pathologically confirmed after surgery and underwent CT within two weeks before surgery were selected. The exclusion criteria were as follows: incomplete clinical data; CT images that were incomplete or of poor quality. A binary logistic regression model was built for analysis. Through univariate and multivariate analysis, CT image features were evaluated to determine the significant differences between GS and GST.

Results: The study population comprised 203 consecutive patients (29 with GS and 174 with GST). There were significant differences in gender distribution (P=0.042) and symptoms (P=0.002). Besides, GST tended to involve the presence of necrosis (P=0.003) and lymph nodes (P=0.003). The area under the curve (AUC) value of unenhanced CT (CTU) was 0.708 [95% confidence interval (CI): 62.10–79.56%], the AUC value of venous phase CT (CTP) was 0.774 (95% CI: 69.45–85.34%), and the AUC value of venous phase enhancement (CTPU) was 0.745 (95% CI: 65.87–83.06%). CTP was the most specific feature, with a sensitivity of 83% and a specificity of 66%. The ratio of long diameter to short diameter (LD/SD) was significantly different (P=0.003). The AUC of the binary logistic regression model was 0.904. Multivariate analysis showed that necrosis and LD/SD were independent factors affecting the identification of GS and GST.

Conclusions: LD/SD was a novel distinguishing feature between GS and non-metastatic GST. In conjunction with CTP, LD/SD, location, growth pattern, necrosis, and lymph node, a nomogram was constructed to predict.

Keywords: Schwannoma; stromal tumor; gastric; computed tomography (CT); nomogram

Submitted Jan 11, 2023. Accepted for publication Mar 21, 2023. Published online Apr 04, 2023.
doi: 10.21037/jgo-23-93
View this article at: https://dx.doi.org/10.21037/jgo-23-93

Introduction

Gastric schwannoma (GS) was a rare benign gastric mesenchymal tumor, accounting for 2.6% of gastric mesenchymal tumors (1). Gastric stromal tumor (GST) was a relatively common malignant gastric tumor that could metastasize. The clinical manifestations of GS and GST were not typical, and sometimes they manifested no obvious symptoms. Generally, only imaging examination could differentiate GS and GST (2,3).

Conventional preoperative imaging diagnostic methods included computed tomography (CT) and endoscopic ultrasonography. For similar morphological characteristics, common CT imaging features were not specific in differentiating GS from non-metastatic GST (4-7). Endoscopic ultrasonography was an invasive examination, which was not suitable for some patients with contraindications; moreover, some others refused to undergo invasive examinations. Patients with GS did not usually experience recurrence after surgery, but GST patients required follow-up to prevent recurrence or metastasis. There was a difference in prognosis between GS and GST (8-10). Preoperative differentiation between GS and GST was helpful to avoid unnecessary psychological pressure on patients with GS (11). Therefore, new CT features were needed to be further studied to discriminate GS and GST. The nomogram constructed by CT features had an advantage in the differential diagnosis of gastric malignant tumors. Further, as multiple CT features were needed to be analyzed to make a comprehensive judgment, a new data model was required.

The purpose of this study was to evaluate the role of a new CT feature in differentiating GS from non-metastatic GST and to establish a visual and data model to improve the differential ability. We present the following article in accordance with the TRIPOD reporting checklist (available at https://jgo.amegroups.com/article/view/10.21037/jgo-23-93/rc).

Highlight box

Key findings

- LD/SD is a novel distinguishing feature between GS and non-metastatic GST.

What is known and what is new?

- New CT features were needed to identify GS and GST.
- In conjunction with CTP, LD/SD, location, growth pattern, necrosis, and lymph node, a visual evaluation can be shown by the model nomogram.

What is the implication, and what should change now?

- Multiple CT features were needed to make a comprehensive judgment, and new data model was required.

Methods

Patient population and study design

The study was conducted in accordance with the Declaration of Helsinki (as revised in 2013). The study was approved by ethics board of The Fourth Hospital of Hebei Medical University (No. 2022KY385) and individual consent for this retrospective analysis was waived. A database of pathology and CT was used for the initial search. "Gastric schwannoma" and "gastric stromal tumor" were utilized as search terms. Consecutive patients from January 2017 to December 2020 were enrolled in this study. The inclusion criteria were as follows: (I) patients were confirmed as having GS or non-metastatic GST by surgery and pathology; (II) a CT examination was performed within 2 weeks before surgery; (III) no treatment had been given before surgery. The initial total study populations before exclusions were 31 for GS and 179 for GST.

The exclusion criteria were as follows: (I) the CT images were incomplete or the stomach was not adequately distended; (II) the tumor was not solitary or the maximum diameter of the tumor was less than 10 mm in the long axis (*Figure 1*).

Clinical data

The following clinical features were recorded: (I) gender, (II) age, and (III) specific clinical symptoms (abdominal distension, abdominal pain, upper gastrointestinal bleeding).

CT acquisition technique

Patients were fasted for six hours and given 800 mL of water before the scan. Unenhanced CT, enhanced arterial phase, and enhanced venous phase scans were performed on all patients. The GE Revolution 128 CT scanner (GE Healthcare, Chicago, IL, USA) was used with a routine slice thickness of 5 mm, 120 kV, 250 kV, and 350 mAs, and the whole abdomen was scanned from the top of the diaphragm to the level of the inferior edge of the pubic symphysis. Enhanced scanning was conducted with nonionic contrast

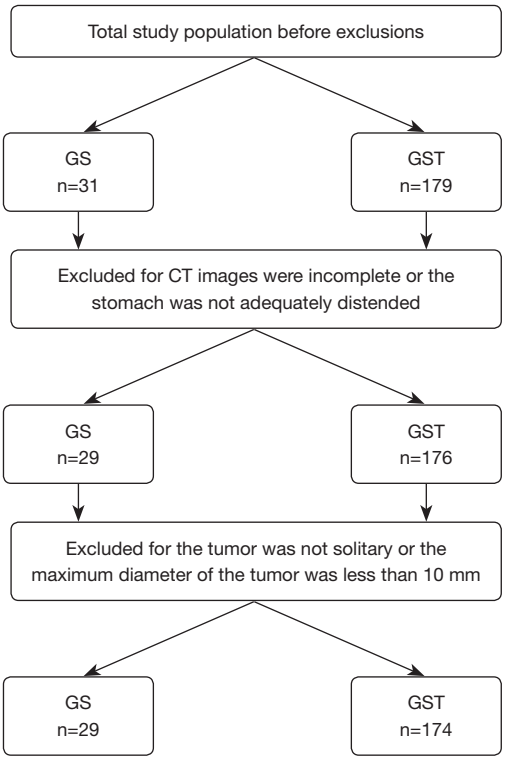

Figure 1 Flowchart of the study. GS, gastric schwannoma; GST, gastrointestinal stromal tumor; CT, computed tomography.

medium (iodine content: 300 mg/mL), injection flow rate (3.0 mL/s), and total contrast medium (100 mL). The arterial phase and venous phase were scanned at 35 seconds and 70 seconds after injection.

CT image analysis

Each feature was analyzed independently by 2 radiologists with 6 and 19 years of respective experience. Both radiologists were blinded to the histological subtypes of the samples. The following CT features were recorded: (I) location of the lesion or mass; (II) contour of the lesion or mass; (III) growth pattern; (IV) peritumoral infiltration; (V) necrosis; (VI) calcification; (VII) surface ulceration; (VIII) the presence of enlarged lymph nodes; (IX) the long diameter (LD); (X) the short diameter (SD); (XI) the ratio of the long diameter to the short diameter (LD/SD); (XII) unenhanced CT value (CTU); (XIII) arterial phase CT value (CTA); (XIV) venous phase CT value (CTP); (XV) arterial phase enhancement value (CTAU); and (XVI) venous phase enhancement value (CTPU).

Necrosis was defined as an unenhanced liquid density

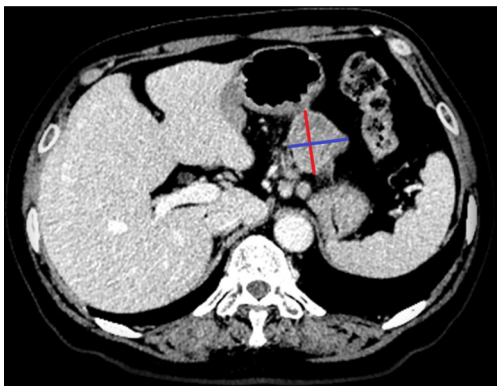

Figure 2 GS in a 64-year-old female. The LD and SD are orthogonal measurements on the axial image. GS, gastric schwannoma; LD, long diameter; SD, short diameter.

in any area, regardless of its size. Lymph nodes with an SD ≥10 mm were considered significantly different. The orthogonal measurements of the LD and SD were performed on the axial image at the largest level of the tumor (*Figure 2*). Besides, the measurement methods of GS and GST were consistent. The measurements of LD and SD were repeated three times, and the average value was recorded. As for attenuation, a circular region of interest (ROI) was placed to exclude areas of necrosis and calcification. If the readers disagreed on any measurements, a decision was made through consultation.

Statistical analysis

All statistical analyses were performed using R version 3.6.3 (The R Foundation for Statistical Computing, Vienna, Austria) and Python version 3.7 (Pythion Software Foundation, Wilmington, DE, USA). The clinical and CT signs were compared using the Mann-Whitney-U test, χ^2 test, and the Student's *t*-test. A binary logistic regression model was built for analysis. Univariate and multivariate analyses were also carried out in this study. Additionally, the receiver operating characteristic (ROC) curve was used to determine the optimal critical value, sensitivity, and specificity of meaningful quantitative CT signs. A P value of 0.05 was considered statistically significant.

Results

Patient population and clinical data

The study population comprised 203 consecutive patients,

Table 1 Clinical characteristics of 203 patients with GS and GST

Clinical characteristics	GS (n=29)	GST (n=174)	P value
Age, mean (SD)	56.345 (10.243)	59.759 (9.496)	0.079
Gender, n (%)			
Male	7 (24.138)	77 (44.253)	0.042
Female	22 (75.862)	97 (55.747)	
Symptom, n (%)			
No	18 (62.069)	57 (32.759)	0.002
Yes	11 (37.931)	117 (67.241)	

GS, gastric schwannoma; GST, gastrointestinal stromal tumor; SD, standard deviation.

including 29 GS patients (7 males and 22 females, with a mean age of 56 years) and 174 GST patients (77 males and 97 females, with a mean age of 59). There were significant differences in gender distribution (P=0.042) and symptoms (P=0.002). The full results are reported in *Table 1*.

CT image analysis

Firstly, the locations of GS and GST were significantly different (P=0.003); predominantly, GS was located in the body [75.9% (22/29)], whereas GST was in the fundus [43.1% (75/174)] and body [43.7% (76/174)]. In addition, the contour of GS tended to be round or oval [65.5% (19/29)], whereas the contour of GST was irregular [59.2% (103/174)]. Moreover, the tumor growth pattern of GS tended to be mixed [65.5% (19/29)], whereas that of GST tended to be endophytic [40.8% (71/174)]. Furthermore, GST tended to have the presence of necrosis (P=0.003) and the presence of lymph nodes (P=0.003).

According to the outcomes of quantitative CT image analysis, the CTU, CTA, CTP, and CTPU of GS were higher than those of GST (P<0.05). Moreover, the LD/SD ratios between GS and GST were also significantly different (P=0.003). The full results are reported in *Table 2*.

CT diagnostic performance

A binary logistic regression model was constructed, and then univariate and multivariate analyses were carried out. According to the analysis results, patients with GS and GST exhibited some significant differences (P<0.05) in the irregular contours [P=0.016, odds ratio (OR) 2.756], mixed growth patterns (P=0.001, OR 0.118), the presence of liver necrosis (P=0.005, OR 3.382), enlarged lymph nodes (P=0.014, OR 0.101), and the values of LD/SD (P=0.014, OR 12.547), CTU (P=0.010, OR 0.938), CTA (P=0.004, OR 0.959), and CTP (P<0.001, OR 0.947), and CTPU (P<0.001, OR 0.956). The full results are reported in *Table 3*.

Binary logistic regression was applied to evaluate the effects of CTU, CTA, CTP, CTPU, LD/SD, location, contour, growth pattern, necrosis, and lymph nodes on the grouping. The area under the curve (AUC) of the model was 0.904 [95% confidence interval (CI): 0.834–0.974], and the prediction effect of the model was good (*Figure 3*). Statistically significant results included the coefficient of variable CTP (0.06; P=0.001), LD/SD (3.411; P=0.017), mixed growth pattern (–2.725; P=0.001), and the presence of an enlarged lymph node (–2.564; P=0.028). Multivariate analysis showed that necrosis and LD/SD were independent factors affecting the identification of GS and GST.

The AUC value of CTU was 0.708 (95% CI: 62.10–79.56%), that of CTP was 0.774 (95% CI: 69.45–85.34%), and that of CTPU was 0.745 (95% CI: 65.87–83.06%). The full outcomes are reported in *Table 4*. CTP was the most specific feature, with a sensitivity of 83% and a specificity of 66%.

The ROC analysis (*Figure 4*) showed that the largest AUC was the CTP (0.774), followed by the CTPU (0.745) and the CTU (0.708); CTP, CTPU, and CTU were significantly continuous variables differentiating GS from GST.

A violin plot was applied to study the continuous variables of CT value and diameter of GS and GST.

We discovered that the CT median attenuation value was universally lower for the GS than that for the GST, no matter whether CTU, CTA, CTP, CTAU, or CTPU, whereas the diameter was universally larger, regardless of whether LD or SD (*Figure 5*).

The violin plot showed that the CT value was universally higher for the GS than for the GST, whereas the diameter was universally shorter.

Discussion

GS is a rare gastric mesenchymal tumor. Generally, it is difficult to differentiate between the clinical manifestations and CT features of GS and GST. Therefore, we compared the CT findings of GS and GST in this study to facilitate a correct differential diagnosis.

Multivariate analysis showed that necrosis and LD/SD

Table 2 CT features of 203 patients with GS or GST

CT findings	GS (n=29)	GST (n=174)	P value
Location, n (%)			
Cardia	1 (3.448)	5 (2.874)	0.003
Fundus	2 (6.897)	75 (43.103)	
Body	22 (75.862)	76 (43.678)	
Antrum	4 (13.793)	18 (10.345)	
Contour, n (%)			
Round/oval	19 (65.517)	71 (40.805)	0.013
Irregular	10 (34.483)	103 (59.195)	
Growth pattern, n (%)			
Endophytic	3 (10.345)	71 (40.805)	<0.001
Exophytic	7 (24.138)	50 (28.736)	
Mixed	19 (65.517)	53 (30.460)	
Peritumoral infiltration, n (%)			
No	28 (96.552)	168 (96.552)	1.000
Yes	1 (3.448)	6 (3.448)	
Necrosis, n (%)			
No	20 (68.966)	69 (39.655)	0.003
Yes	9 (31.034)	105 (60.345)	
Calcification, n (%)			
No	26 (89.655)	141 (81.034)	0.260
Yes	3 (10.345)	33 (18.966)	
Surface ulceration, n (%)			
No	17 (58.621)	85 (48.851)	0.330
Yes	12 (41.379)	89 (51.149)	
Enlarged lymph node, n (%)			
No	26 (89.655)	172 (98.851)	0.003
Yes	3 (10.345)	2 (1.149)	
CTU, mean (SD)	36.679 (5.606)	32.387 (8.315)	0.001[a]
CTA, median (IQR)	55.600 (49.300, 62.100)	48.200 (41.000, 57.600)	0.001[b]
CTP, median (IQR)	73.900 (69.700, 88.100)	61.600 (52.000, 72.600)	<0.001[b]
CTAU, median (IQR)	19.100 (14.100, 24.000)	14.600 (9.200, 24.300)	0.054[b]
CTPU, median (IQR)	43.200 (31.200, 50.900)	28.900 (21.000, 37.300)	<0.001[b]
LD, median (IQR)	35.100 (28.900, 44.200)	43.000 (26.000, 57.000)	0.310[b]
SD, median (IQR)	27.100 (21.400, 34.900)	31.000 (18.400, 41.900)	0.738[b]
LD/SD, median (IQR)	1.244 (1.140, 1.351)	1.380 (1.240, 1.567)	0.003[b]

[a], *t* test, [b], Mann-Whitney-U test. CT, computed tomography; GS, gastric schwannoma; GST, gastrointestinal stromal tumor; CTU, CT value of unenhanced; CTA, CT value of arterial phase; CTP, CT value of venous phase; CTAU, arterial phase enhancement value; CTPU, venous phase enhancement value; LD, long diameter; SD, short diameter; LD/SD, the ratio of long diameter to short diameter; IQR, interquartile range.

Table 3 Analysis of 203 patients with GS and GST

CT features	N	OR	95% CI	P value
CTU	203.0	0.938	(0.894, 0.985)	0.010
CTA	203.0	0.959	(0.932, 0.987)	0.004
CTP	203.0	0.947	(0.925, 0.971)	<0.001
CTAU	203.0	0.977	(0.948, 1.007)	0.132
CTPU	203.0	0.956	(0.934, 0.979)	<0.001
LD	203.0	1.014	(0.995, 1.033)	0.146
SD	203.0	1.007	(0.984, 1.030)	0.568
LD/SD	203.0	12.547	(1.652, 95.286)	0.014
Location				
Cardia	6.0			
Fundus	77.0	7.500	(0.577, 97.551)	0.124
Body	98.0	0.691	(0.077, 6.228)	0.742
Antrum	22.0	0.900	(0.081, 9.970)	0.932
Contour				
Round/oval	90.0			
Irregular	113.0	2.756	(1.210, 6.279)	0.016
Growth pattern				
Endophytic	74.0			
Exophytic	57.0	0.302	(0.074, 1.224)	0.094
Mixed	72.0	0.118	(0.033, 0.419)	0.001
Peritumoral infiltration				
No	196.0			
Yes	7.0	1.000	(0.116, 8.623)	>0.999
Necrosis				
No	89.0			
Yes	114.0	3.382	(1.455, 7.859)	0.005
Calcification				
No	167.0			
Yes	36.0	2.028	(0.579, 7.106)	0.269
Surface ulceration				
No	102.0			
Yes	101.0	1.483	(0.669, 3.290)	0.332
Lymph node				
No	198.0			
Yes	5.0	0.101	(0.016, 0.632)	0.014

GS, gastric schwannoma; GST, gastrointestinal stromal tumor; CT, computed tomography; CTU, CT value of unenhanced; CTA, CT value of arterial phase; CTP, CT value of venous phase; CTAU, arterial phase enhancement value; CTPU, venous phase enhancement value; LD, long diameter; SD, short diameter; LD/SD, the ratio of long diameter to short diameter.

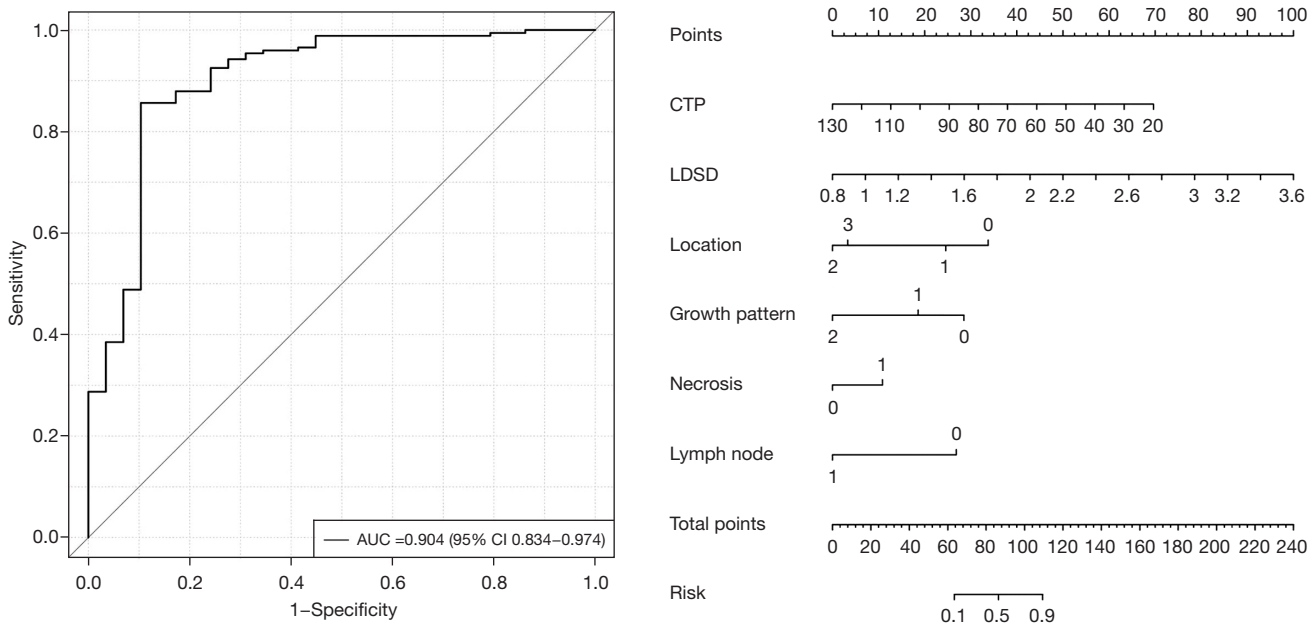

Figure 3 The ROC curve and nomogram of the model. ROC, receiver operating characteristic; AUC, area under the curve; CTP, venous phase computed tomography value; LDSD, the ratio of long diameter to short diameter.

Table 4 AUC, sensitivity, specificity, and cut-off of significant CT features for differentiating GS from GST

CT features	AUC	Optimal boundary value	Sensitivity	Specificity	Cut-off
CTU	0.708	0.402	0.793	0.609	33.400
CTA	0.686	0.379	0.897	0.483	47.600
CTP	0.774	0.489	0.828	0.661	66.900
CTAU	0.612	0.305	0.862	0.443	12.200
CTPU	0.745	0.448	0.966	0.483	27.300

AUC, area under the curve; GS, gastric schwannoma; GST, gastrointestinal stromal tumor; CT, computed tomography; CTU, CT value of unenhanced; CTA, CT value of arterial phase; CTP, CT value of venous phase; CTAU, arterial phase enhancement value; CTPU, venous phase enhancement value.

were independent factors affecting the identification of GS and GST. Although the role of necrosis had been reported in a study (3), LD/SD had not been seriously considered as a meaningful indicator of differentiation. Our study also revealed that the LD/SD of GS was likely to be lower than that of GST. LD/SD can not only reflect the data relationship between LD and SD but also be measured easily. Hence, LD/SD is an index worth popularizing. A nomogram was drawn to visualize the predictive model that distinguishes GS from GST.

Most of the 29 cases with GS were female, which was consistent with the study of Wang *et al.* (12). GS is usually diagnosed by a routine endoscopic physical examination. In our study, the gastric body had the most GS (75.9%), followed by the antrum (13.8%), which was similar to previous research by Wang *et al.* (13). In contrast, among the 174 subjects with GST, 75 (43.1%) cases were located in the fundus of the stomach and 76 (43.7%) in the body of the stomach. Briefly, in the cases of these 2 types of tumors, stromal tumors tended to be diagnosed in the fundus of the stomach. Additionally, the GS was round or oval in 19 cases (65.5%), and the shape of the GST was irregular in 103 cases (59.2%). In terms of growth pattern, GS was mostly endophytic and exophytic mixed type in 19 cases (65.5%),

whereas GST was mostly exophytic in 71 cases (40.8%). The above outcomes in our study were similar to previous research by Choi *et al.* (14). Furthermore, 3 (10.3%) of the 29 cases of GS had lymph nodes, but only 2 (1.1%) cases of GST had lymph nodes, which was consistent with previous research by Choi *et al.* (15).

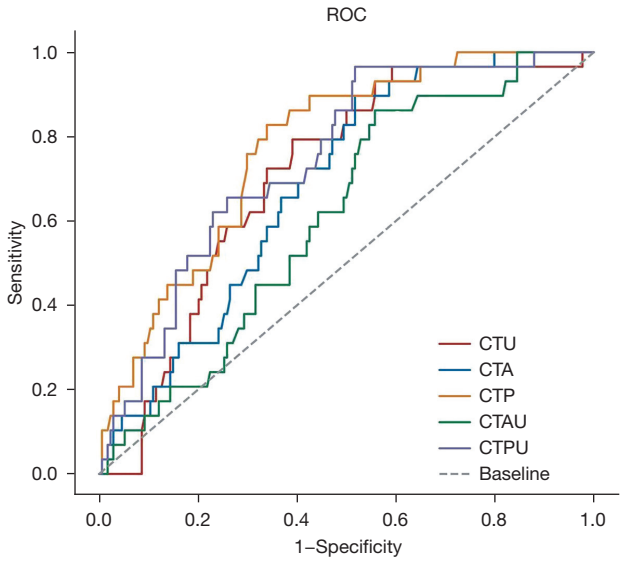

Figure 4 ROC curves of CT values to differentiate GS from GST. ROC, receiver operating characteristic; CT, computed tomography; GS, gastric schwannoma; GST, gastrointestinal stromal tumor; CTU, CT value of unenhanced; CTA, CT value of arterial phase; CTP, CT value of venous phase; CTAU, arterial phase enhancement value; CTPU, venous phase enhancement value.

On the one hand, the CT values of CTU, CTA, and CTP of GS were higher than those of GST, which was similar to previous research by Liu *et al.* (16). On the other hand, both CTAU and CTPU exhibited a higher degree of enhancement in GS than in GST (especially CTPU). Besides, ROC analysis showed that CTP was more efficient in discriminating GS and GST (AUC = 0.774), followed by the CTPU (AUC = 0.745) and the CTU (AUC = 0.708). To sum up, CTU, CTP, and CTPU have a high diagnostic value for grouping. Our results were in accordance with a previous study by Chen *et al.* (17). The enhancement degree of most GS cases in the venous phase was higher than that of GST, which was consistent with the study of Wang *et al.* (13). Due to the malignant potential of GST, the degeneration of tumor cells is easier, and the degree of enhancement of GST is decreased (18). The AUC was best among the predictors related to individual CT values when the CTP cutoff value was 66.9.

In this study, a binary logistic regression model was constructed to evaluate the effects of CTU, CTA, CTP, CTPU, LD/SD, location, contour, growth pattern, necrosis, and the presence of enlarged lymph nodes on the grouping. The AUC of this model was 0.9, indicating that a better differential diagnostic effect could be achieved by constructing a multi-factor model. Multivariate analysis also

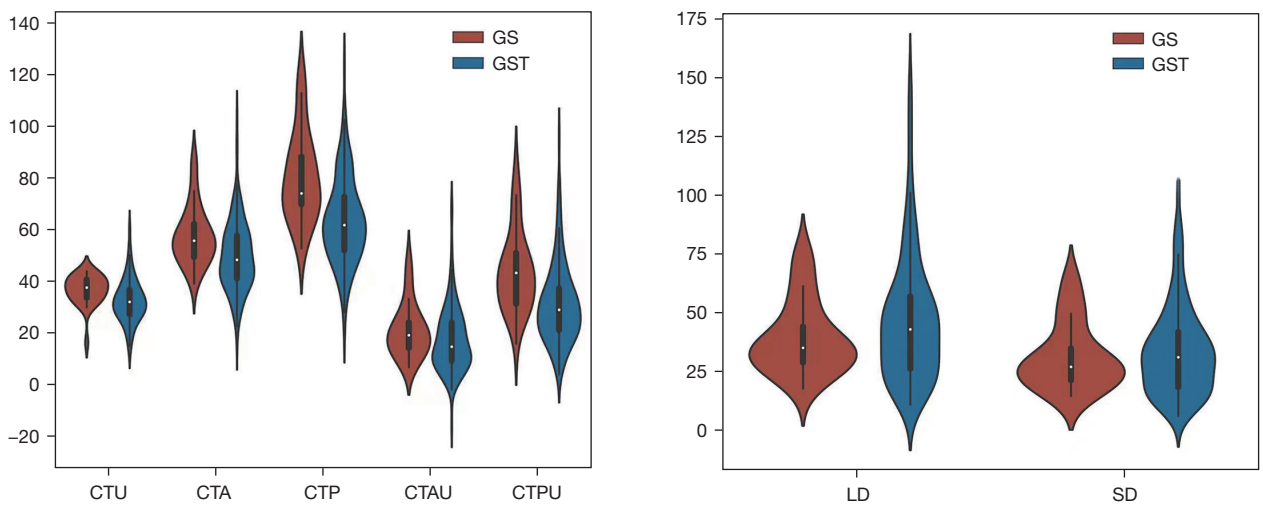

Figure 5 Violin plot for computed tomography values between GS and GST. The Y-axis represented computed tomography value. GS, gastric schwannoma; GST, gastrointestinal stromal tumor; CTU, CT value of unenhanced; CTA, CT value of arterial phase; CTP, CT value of venous phase; CTAU, arterial phase enhancement value; CTPU, venous phase enhancement value; LD, long diameter; SD, short diameter.

revealed that necrosis and LD/SD were independent factors affecting the identification of GS and GST. To the best of our knowledge, the diagnostic value of LD/SD has not been reported in the literature before.

Several limitations in our study cannot be ignored. First, this was a retrospective, single-institution study. Secondly, we excluded patients with multiple gastric tumors. Thirdly, the study only included GS and GST.

Conclusions

LD/SD represents a novel distinguishing feature between GS and non-metastatic GST. In conjunction with CTP, LD/SD, location, growth pattern, necrosis, and lymph nodes, a visual evaluation can be shown by the model nomogram.

Acknowledgments

Funding: None.

Footnote

Reporting Checklist: The authors have completed the TRIPOD reporting checklist. Available at https://jgo.amegroups.com/article/view/10.21037/jgo-23-93/rc

Data Sharing Statement: Available at https://jgo.amegroups.com/article/view/10.21037/jgo-23-93/dss

Conflicts of Interest: All authors have completed the ICMJE uniform disclosure form (available at https://jgo.amegroups.com/article/view/10.21037/jgo-23-93/coif). The authors have no conflicts of interest to declare.

Ethical Statement: The authors are accountable for all aspects of the work in ensuring that questions related to the accuracy or integrity of any part of the work are appropriately investigated and resolved. The study was conducted in accordance with the Declaration of Helsinki (as revised in 2013). The study was approved by ethics board of The Fourth Hospital of Hebei Medical University (No. 2022KY385) and individual consent for this retrospective analysis was waived.

References

1. Tao LP, Huang EJ, Li P, et al. Schwannoma of stomach: a clinicopathologic study of 12 cases. Int J Clin Exp Pathol 2018;11:1679-83.
2. Lyros O, Schickel S, Schierle K, et al. Gastric schwannoma: rare differenzial diagnosis of acute upper gastrointestinal (GI) bleeding. Z Gastroenterol 2017;55:761-5.
3. Lin YN, Chen MY, Tsai CY, et al. Prediction of Gastric Gastrointestinal Stromal Tumors before Operation: A Retrospective Analysis of Gastric Subepithelial Tumors. J Pers Med 2022;12:297.
4. Hu J, Liu X, Ge N, et al. Role of endoscopic ultrasound and endoscopic resection for the treatment of gastric schwannoma. Medicine (Baltimore) 2017;96:e7175.
5. Chen W, Cai G. Endoscopic ultrasound-guided fine-needle aspiration biopsy of gastric schwannoma: Cytomorphologic features and diagnostic pitfalls. Diagn Cytopathol 2019;47:1218-22.
6. Lee MW, Kim GH. Diagnosing Gastric Mesenchymal Tumors by Digital Endoscopic Ultrasonography Image Analysis. Clin Endosc 2021;54:324-8.
7. Kim YH, Kim GH, Kim KB, et al. Application of A Convolutional Neural Network in The Diagnosis of Gastric Mesenchymal Tumors on Endoscopic Ultrasonography Images. J Clin Med 2020;9:3162.
8. Lauricella S, Valeri S, Masciana G, et al. What About Gastric Schwannoma? A Review Article. J Gastrointest Cancer 2021;52:57-67.
9. Zhai YQ, Chai NL, Li HK, et al. Endoscopic submucosal excavation and endoscopic full-thickness resection for gastric schwannoma: five-year experience from a large tertiary center in China. Surg Endosc 2020;34:4943-9.
10. Zhai YQ, Chai NL, Zhang WG, et al. Endoscopic versus surgical resection in the management of gastric schwannomas. Surg Endosc 2021;35:6132-8.
11. Seven G, Silahtaroglu G, Kochan K, et al. Use of Artificial Intelligence in the Prediction of Malignant Potential of Gastric Gastrointestinal Stromal Tumors. Dig Dis Sci 2022;67:273-81.
12. Wang J, Zhang W, Zhou X, et al. Simple Analysis of the

Computed Tomography Features of Gastric Schwannoma. Can Assoc Radiol J 2019;70:246-53.
13. Wang W, Cao K, Han Y, et al. Computed tomographic characteristics of gastric schwannoma. J Int Med Res 2019;47:1975-86.
14. Choi JW, Choi D, Kim KM, et al. Small submucosal tumors of the stomach: differentiation of gastric schwannoma from gastrointestinal stromal tumor with CT. Korean J Radiol 2012;13:425-33.
15. Choi YR, Kim SH, Kim SA, et al. Differentiation of large (≥5 cm) gastrointestinal stromal tumors from benign subepithelial tumors in the stomach: radiologists' performance using CT. Eur J Radiol 2014;83:250-60.
16. Liu J, Chai Y, Zhou J, et al. Spectral Computed Tomography Imaging of Gastric Schwannoma and Gastric Stromal Tumor. J Comput Assist Tomogr 2017;41:417-21.
17. Chen Z, Yang J, Sun J, et al. Gastric gastrointestinal stromal tumours (2-5 cm): Correlation of CT features with malignancy and differential diagnosis. Eur J Radiol 2020;123:108783.
18. Akahoshi K, Oya M, Koga T, et al. Current clinical management of gastrointestinal stromal tumor. World J Gastroenterol 2018;24:2806-17.

(English Language Editor: J. Jones)

Cite this article as: Gu X, Li Y, Shi G. Identification of gastric schwannoma and non-metastatic gastric stromal tumor by CT: a single-institution retrospective diagnostic test. J Gastrointest Oncol 2023;14(2):922-931. doi: 10.21037/jgo-23-93

